**PAPER • OPEN ACCESS**

# Ranking materials technologies by limiting characteristics of heat-resistant alloys and their longevity in the problems of import substitution

To cite this article: F I Murataev *et al* 2019 *IOP Conf. Ser.: Mater. Sci. Eng.* **570** 012070

IOP Conf. Series: Materials Science and Engineering **570** (2019) 012070 doi:10.1088/1757-899X/570/1/012070

# Ranking materials technologies by limiting characteristics of heat-resistant alloys and their longevity in the problems of import substitution

**F I Murataev[1], E R Galimov[1] and N Ya Galimova[1]**

[1]Kazan national research technical university named after A.N. Tupolev, K. Marx street 10, Kazan, 420111, Tatarstan, Russian Federation

kstu-material@mail.ru

**Abstract.** The structural strength properties determined by the true stress-deformation diagram and the fatigue characteristics of materials at combined action (tension and bending) under the conditions of temperature change are used to substantiate materials and technologies. The domestic alloy is suggested as an alternative to imported heat-resistant alloy IN-738LC used to manufacture the turbine rotor blades of stationary gas turbine plants (GTP). Expressions to determine the fatigue characteristics according to the criteria of structure stability are presented.

## 1. Introduction
The operating practice of stationary GTP shows that their parameters temperature, turbine speed and the actual loads in comparison with transport gas turbine engines (GTE) (in particular aviation) are more gentle [1, 2]. In this regard, some companies, for example, “MAN” use cheaper materials in the manufacturing of gas turbines [2-5].

## 2. Body text
The analysis of turbine rotor blades structure made of CrNi65WMoTiAl alloy and IN-738LC according to the variants of their state after bench-tests and operating time of GTP is performed in order to identify the damage laws and to use the domestic alloys, for example in the repair of imported products. The microcracks with a size of 3…7 μm were detected in the alloy IN-738LC after operating time (Fig. 1, a), cracks [2-4, 6, 9], fatigue striations and breakdown of carbide $(Cr, Mo, W)_6C$ into the σ-phase were detected in the CrNi65WMoTiAl alloy (Fig. 1, b). Table 1 shows the comparative data of the element-by-element composition of the blade material under study.

**Table 1.** The chemical composition of the alloys under study (in volume %)

| Alloy grade | W | Mo | Zr | Co | Nb | Ta | Ni | Cr | Ti | Al |
|---|---|---|---|---|---|---|---|---|---|---|
| IN-738LC [1], USA | 2.6 | 1.7 | 0.05 | 8.5 | 0.9 | 1.7 | 61 | 16 | 3.4 | 3.4 |
| CrNi65WMoTiAl, Russian Federation | 9.2 | 4.0 | 0 | 0 | 0 | 0 | 65 | 16 | 1.4 | 1.4 |

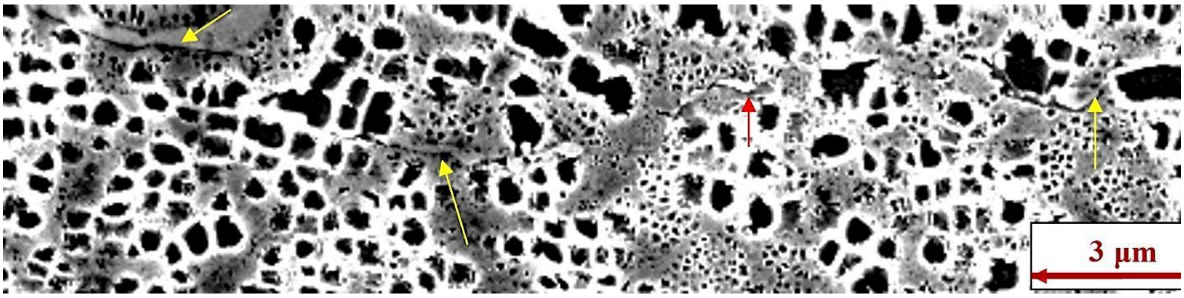


a

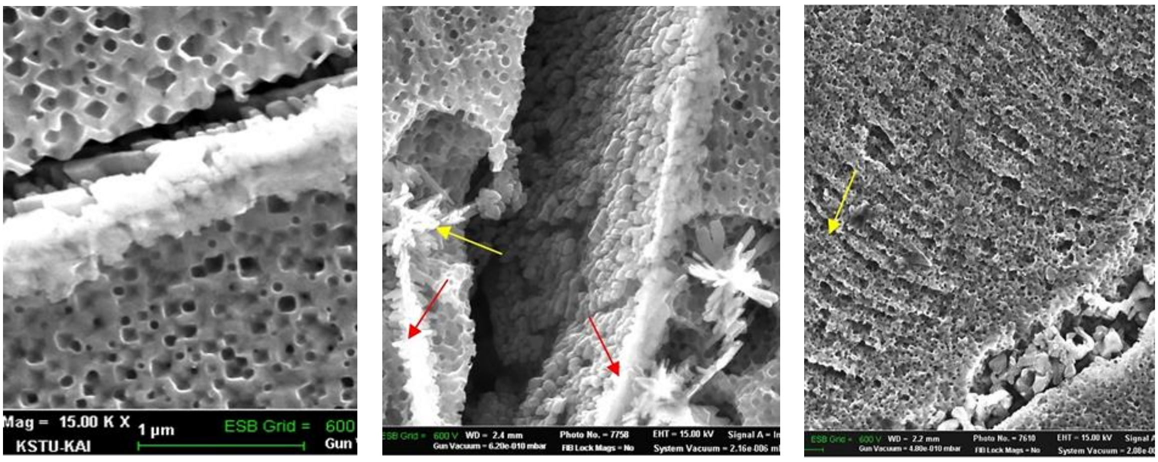


b

**Figure 1.** Metal degradation after operating time in the alloy IN-738LC (a) and in the alloy CrNi65WMoTiAl (b): cracks and breakdown of $(Cr,Mo,W)_6C$ into brittle σ-phase [2, 3, 6] and fatigue striations (right).

Structural damage of the alloy (SDA) expressed by the values of the standard deviations of the reflected ultrasonic signals [2-4, 9] over the sections of the blade airfoil cross-sections, is used to assess the degree of metal degradation. The dependencies (1) – (8) are used for the analysis of IN-738LC alloy damage, the dependence (9) – for the alloy CrNi65WMoTiAl:

$$SDA = 42.896 + 2.4382 \cdot \gamma'_{b}, \quad (1)$$

- from the size of the grain-boundary **γ′**-phase;

$$SDA = 64.758 - 1.8067 \cdot \gamma'_{eu}, \quad (2)$$

- from the size of the eutectic **γ′**-phase (fig. 2);

$$SDA = 41.262 + 0.925 \cdot (Ti,Nb,W) \cdot C; \quad (3)$$

$$SDA = 41.262 + 0.925 \cdot (Ti,Nb,Ta) \cdot C; \quad (4)$$

$$SDA = 47.551 + 1.2171 \cdot \lambda_{II}; \quad (5)$$

$$SDA = 61.68 - 60.50 \cdot (Ta+Co)/Ni; \quad (6)$$

$$SDA = 57.73 - 81.41 \cdot (Mo+Ta)/Ni; \quad (7)$$

$$SDA = 58.49 - 107.3 \cdot (Ta+Nb)/Ni; \quad (8)$$

$$SDA = 67.554 - 0.255 \cdot \Sigma AE \text{ in } M_6C+\gamma', \quad (9)$$

where ΣAE – (+) alloying elements.

The ability of blades metal to resist fatigue at combined action (tension and bending) under conditions of temperature change is determined according to the generalized condition of the limiting amplitudes of the high-frequency component ($\sigma_{a2}$) of the form [8, 10, 13]:

$$\frac{\sigma_{a2}}{\sigma_{-1}} = 1 - R_1 \left( \frac{\sigma_{\max_1}}{\sigma_{R_1}} \right)^{n_1} - \left(1 - R_1\right) \left( \frac{\sigma_{\max_1}}{\sigma_{R_1}} \right)^{n_2} . \quad (10)$$

Equivalent biaxial stresses are equal to [13]:

$$\sigma_{\mathrm{Re}1} = \sigma_{X1}(1 - \chi_m) + \chi_m(\sigma_{X1}^2 + \sigma_{Y1}^2 - 2\mu\sigma_{X1}\sigma_{Y1})^{0.5} . \quad (11)$$

$$n_2 = B_1 + B_2 \frac{\sigma_{\max_1}}{\sigma_{R_1}} - B_3 \frac{E_k}{E} + B_4 \frac{\mu}{\Psi} + B_5 \frac{m^{(0)}\Psi}{\delta} , \quad (12)$$

where $\sigma_{\max 1} = \sigma_A + \sigma_C$ – sum of actual and thermal stresses; properties are taken at $t_{\max}$ (in $^{O}$C).

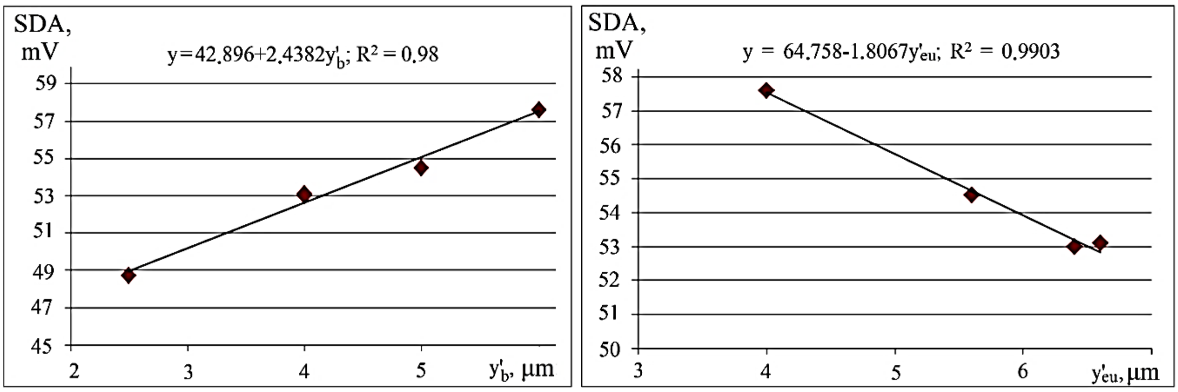


**Figure 2.** Size effect of the hardening phase located at the dendrites boundary and in the eutectic

Ilyushin's relative module [13]:

$$\mathrm{E_k} = \mathrm{E_k} / \mathrm{E} = \left[ 1 + \frac{\mathrm{E}}{\mathrm{S_k}} \ln\left( \frac{1}{1-\psi} \right) \right]^{-1.0} . \quad (13)$$

Strain-hardening coefficient [10-13].

$$\mathrm{m}^{(0)} = 0.75 \ln \frac{\mathrm{S_k}}{\sigma_{0.2}} \left\{ \ln\left[ \left( \frac{\sigma_{0.2}}{\mathrm{E}} + 0.2 \cdot 10^{-2} \right)^{-1.0} \left( \frac{\mathrm{S_k}}{\mathrm{E}} + \ln \frac{1}{1-\psi} \right) \right] \right\}^{-1.0} . \quad (14)$$

According to the data of simulation modeling (SM) when substantiating the materials choice, the preference should be given to the structural state of alloys with higher values of the characteristics $S_K$, $m^{(0)}$, $\psi$. and smaller $E_K$. At dual-frequency loads the decrease of fatigue life ($N/N_1$) is controlled by expressions (11, 12, and 16) depending on the inclination angle of the fatigue curve (γ) in the low-cycle fatigue life region ($N_1$) taking into account the acting stresses ($\sigma_{\max 1}$), values of equivalent stresses ($\sigma_{\mathrm{Re}1}$), characteristics of strength and plasticity in (12) at the maximum temperature *f*n(t) according to the condition [13]:

$$N_1 / N = 1 - \left(\sigma_{a_2} / \sigma_{-1}^{t}\right)^{\gamma/n(t)} . \quad (15)$$

The simulation modeling and fatigue tests of CrNi77TiAlB (EI437-BU) and 13Cr11Ni2W2MoV steel (EI961-Sh) were performed under complex thermal and force actions on the material [13] to check the calculated dependences (10-15). When the tensile and bending stresses in the samples (Fig. 3) are combined with the stresses from thermal cycling within the temperature range from 100 to 400$^{o}$C (tvar 100...400$^{o}$C) it can be seen (Fig. 4) that the experimental and calculated data obtained by the author [13] are in good agreement.

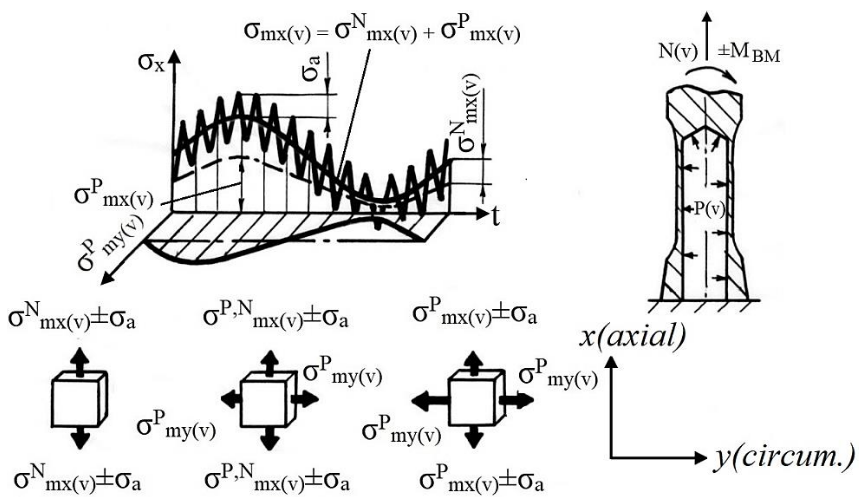


**Figure 3.** Schemes of combined action of tension (N), pressure (P) and bending ($\sigma_a$) at testing of samples

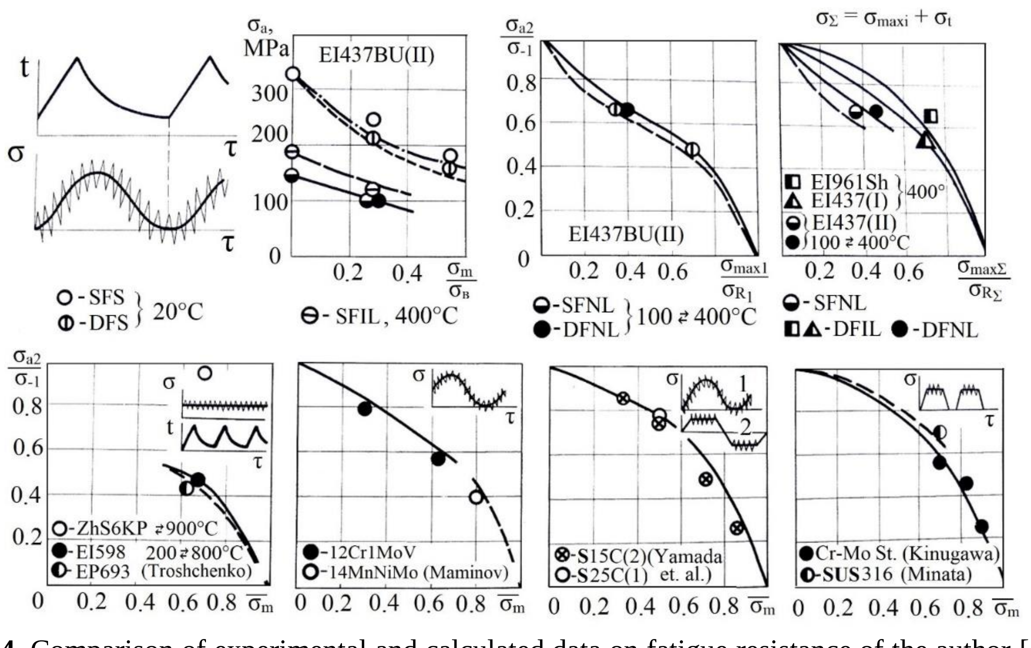


**Figure 4.** Comparison of experimental and calculated data on fatigue resistance of the author [13] and data of Troshchenko V T [12], Maminov A S, Yamada T, Minata H [16], Kinugawa MSFS – single frequency stress, DFS – dual-frequency stress, SFIL – single-frequency isothermal loading, SFNL – single-frequency non-isothermal loading, DFIL – dual-frequency isothermal loading, DFNL – dual-frequency non-isothermal loading

Other results are obtained by Maminov A.S. (at KAI), at the Institute for Problems of Strength National Academy of Sciences of Ukraine (at t var = 200...900 and 200…800$^o$C) by Troshchenko V T [12] and at the University of Kyoto (Japan at t var = 200...700$^o$C) [16]. The disks of the third stage of the GTE turbine are exposed to severe plastic deformation due to stress concentration in the zone of the hub bolt holes. Because of the constraint of the complex stress-strain state (SSS) [7, 11] and the action of high stresses, significant exhaustion of the plasticity reserve – the relative reduction up to 56% (Fig. 5) – takes place at operating and bench-tests time ~ 10000 hours. Since this process is influenced by both operating [14] and technological heredity, the enterprises have regulations on fixing the current level of properties (CLP) and properties of the initial level (PIL).

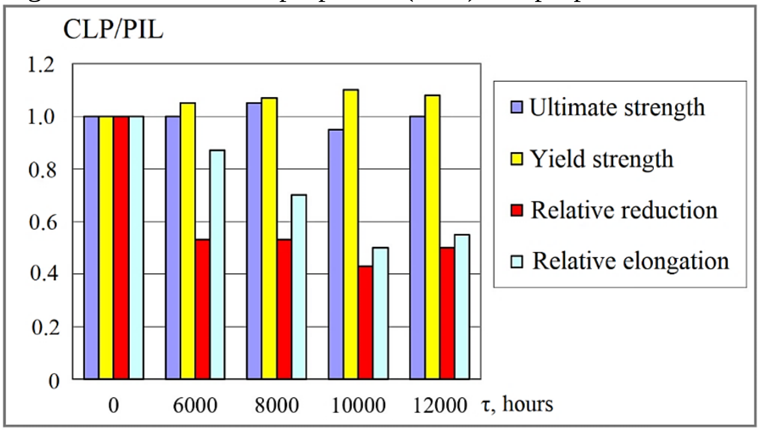


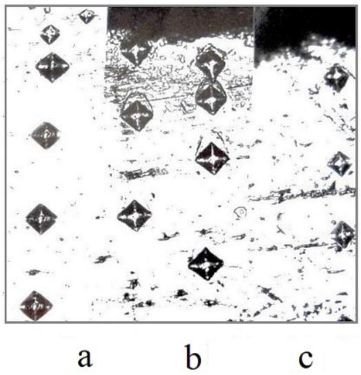


**Figure 5**. Changes in properties (CLP/PIL) of the CrNi73MoNbTiAl alloy with operating time of disks and measurement of metal microhardness at the hub holes according to the variants: after operation – (a), Restorative heat treatment (RHT) – (b), and operation + RHT – (c)

An increase in the hardness $H_{100}$ of the deformed metal of the hub holes surface by 40…60% (Fig. 5, a) was established [12-15]. The turbine disks under repair are exposed to RHT in the "recovery of metals" mode – as a part of the equilibrium solidus temperature ($T_{OT}$ ~ $0.35T_{RS}$). As a result, the hardness and plasticity ($\psi$) are completely restored to the level of PIL and higher including that after repeated bench-tests time (Fig. 5, b and c). Thus, in this part of the research, the criteria for maintainability and assessment of the repair efficiency were established using the available and informative characteristics $H_{100}$ and $\psi$. This made it possible to repair the turbine disks in engines conducting the RHT instead of replacing them.

The heat treatment modes were optimized with respect to the microstructure and microindentation characteristics performed on the SHIMADZU DUH-211S hardness tester by the Berkovich pyramid. The only indicator (out of 14 analyzed) consistent with the properties of the structural strength of materials is the difference in depth from the indentation of the indenter under constant load, according to the instruction – "creep under constant load – CIT". In our opinion, a more accurate name of this characteristic is the available indentation plasticity (AIP) on the upper area of the diagram: indentation depth – endurance – unloading. Figure 6 illustrates the level of this property by the extent of the areas before indentation of the pyramid according to variants (a-c) of thermal treatment of 13Cr11Ni2W2MoV steel samples according to table 2. From the presented data a good agreement of structure's characteristics and the property $\psi$ with the AIP indicator can be seen.

**Table 2.** Influence of heat treatment on the steel mechanical properties including the AIP indicator

| No. of variant | States of 13Cr11Ni2W2MoV steel | | $HV_{100*}$ | $\sigma_B$ | $\psi$ | AIP |
|---|---|---|---|---|---|---|
| | Double hardening | Tempering | MPa*$10^{-1}$ | MPa | % | |
| 1 (a) | After operation | | ~370 | 1180 | 41 | 6.18 |
| 2 (b) | (1020 + 1000) °C – oil | 560°C | 572 | 1540 | 55 | 8.78 |
| 3 (c) | (1020 + 1000) °C - oil | 640°C | 380 | 1230 | 72 | 23.78 |

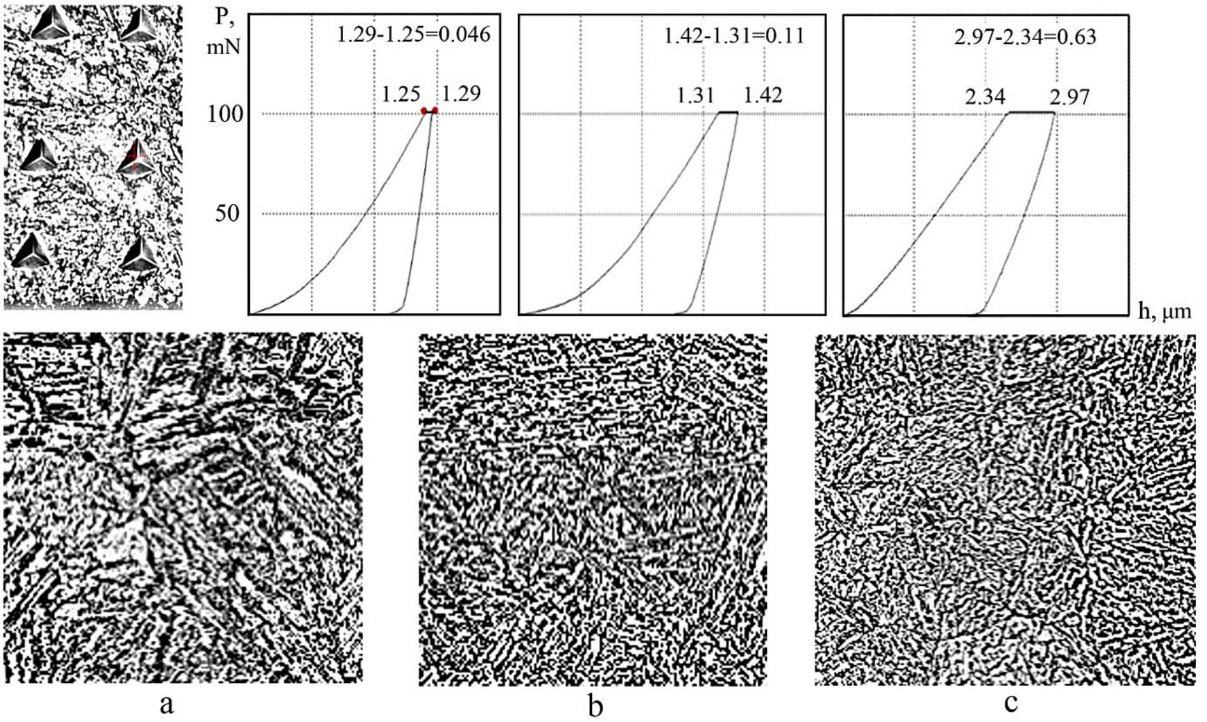


**Figure 6.** Determination of available indentation plasticity and structural states of 13Cr11Ni2W2MoV steel corresponding to variants of heat treatment (a-c) table 2

Thus, as a result of conducted complex studies the technologies and structural states of materials that provide functionality and long-term operation of complex equipment are revealed. For this purpose, the characteristics of the true deformation curve, the estimated fatigue life, the influence of operating and bench-test times on the parameters of heat-resistant alloy structure (its damageability) are used. In addition, the paper proposes the criterion of "available indentation plasticity" which allows adequately and reliably substantiating the adoption of technological decisions, the choice of the material including the identification of the advantages of the home-grown technologies without destroying the metal.

## 3. Conclusions

The shape transformation of the globular and cube-shaped particles of the hardening $\gamma'$-phase into geometry that is irregular (relief) along the perimeter and their crushing indicates the damage of the alloy structure (up to SDA levels = 0.53…0.57 mV) when microcracks can form in the blade. Increasing the amount of Cr, Ta, Mo, W, Co and decreasing the amount of Ti, Ni in the $\gamma'$-phase of the IN-738LC alloy increases the fatigue resistance of the rotor blades with a cast structure. Increasing the sum of alloying elements in $(Cr,Mo,W)_6C$ and $\gamma'$-phase of the CrNi65WMoTiAl alloy increases fatigue resistance of the turbine rotor blades. The increase in the distance between the axes of the second-order dendrites ($\lambda_{II}$) increases the damageability of the IN-738LC alloy. The possibility of repairing the disks made of the CrNi73MoNbTiAl alloy using the RHT in the recovery mode ($T \sim 0.35T_{RS}$) was confirmed. Effective technologies and structural states of materials were identified namely preference should be given to the states of CrNi65WMoTiAl and CrNi73MoNbTiAl alloys with higher values of $S_K$, $m^{(0)}$, $\psi$ and smaller – $E_K$, $H_{100}$ ensuring functionality and long-term operation of complex equipment.

## References

IOP Conf. Series: Materials Science and Engineering **570** (2019) 012070 doi:10.1088/1757-899X/570/1/012070

[1] Sims C T and Stoloff N S 1995 *Translation Superalloys II: High-temperature materials for aerospace and industrial power* (Moscow: Metallurgiya) 384 p
[2] Murataev F I and Murataev A F 2016 Study of damageability of metal of GTP compressor disks *Vestnik of KSTU* number 4 pp 31-35
[3] Murataev F I, Saitkulov V G, Khusnutdinov Sh N and Trifonov A A 2014 Regularities of composition, structure, and damageability of turbine blades metal after bench-test and operating time *Vestnik of KSTU* number 2 pp 74-78
[4] Murataev F I and Murataev A F 2015 Influence of composition and morphology of intermetallic phase of IN-738LC alloy on damageability of gas turbine blades *Vestnik of KSTU* number 3 pp 43-48
[5] Tarasenko L V 2005 *Heat-resistant cast nickel alloys of equiaxed crystallization* (Moscow, Herald of the Bauman Moscow State Technical University) pp 50
[6] Murataev F I and Klabukov M A 2014 Study of regularities of structure and fatigue damageability of cast blades made of IN738-LC alloy *Vestnik of KSTU* number 3 pp 107-109
[7] Arthur J McEvily 2002 *Metal Failures: Mechanisms, Analysis, Preventions* (Moscow: Tekhnosfera) 416 p
[8] Murataev F I and Zharzhanazi M A 2013 Provision of structural strength of titanium alloys according to criteria of ultimate plasticity and fatigue resistance *Vestnik of KSTU* number 1 pp 50-54
[9] Kantyukov R R, Tameev I M, Saitkulov V G, Khusnutdinov Sh N, Murataev F I et. al. 2014 Application of ultrasonic nanoscopy method to control the blades of gas turbine engines of gas compressor units in production and operation *Proceedings of the XX International Congress «CITOGIC 2014» «New high technologies of gas, oil industry, energetics and communications»* (Kaliningrad: publishing house Ekonomika) pp 178-189
[10] Murataev F I and Khakimov S Sh 2014 Substantiation of microstructure and properties relationships of titanium alloys for prediction problems of fatigue resistance *Vestnik of KSTU* number 3 pp 110-113
[11] Shkanov I N, Braude N Z and Murataev F I 1982 Model of optimization of basic mechanical properties with respect to static and fatigue strength criteria in complex stress state conditions *Soviet Aeronautics* vol 25 Issue 1 pp 79-84
[12] Troshchenko V T 1981 *Deformation and destruction of metals under high-cycle loading* (Kiev: Naukova Dumka) 344 p
[13] Shkanov I N and Murataev F I 1996 Study of fatigue resistance criteria in modeling problems of operating and technological states of engine elements *Izv. VUZ. Aviatsionnaya Tekhnika* number 4 pp 58-61
[14] Murataev F I and Shkanov I N 1999 Substantiation of processing technology of compressor disks according to characteristics of static and cyclic deformation *Izv. VUZ. Aviatsionnaya Tekhnika* number 1 pp 43-47
[15] Murataev F I and Murataev A F 2016 Determination of rupture source of planetary reduction gearbox of HYUNDAI-R170 excavator *Vestnik of KSTU* number 3 pp 87-90
[16] Hideo Minata 1994 Estimation of fatigue life under conditions of varying average stresses and temperature by the example of GTP disk *Departmental special-purpose programme* No 38118 p 26